Published in final edited form as:
Science. 2013 November 29; 342(6162): 1104–1107. doi:10.1126/science.1242321.

Phycobilisomes Supply Excitations to Both Photosystems in a Megacomplex in Cyanobacteria

Haijun Liu[1,2], **Hao Zhang**[2,3], **Dariusz M. Niedzwiedzki**[2], **Mindy Prado**[1,2], **Guannan He**[2,3], **Michael L. Gross**[3], and **Robert E. Blankenship**[1,2,3,*]

[1]Department of Biology, Washington University in St. Louis, St. Louis, MO 63130, USA

[2]Photosynthetic Antenna Research Center, Washington University in St. Louis, St. Louis, MO 63130, USA

[3]Department of Chemistry, Washington University in St. Louis, St. Louis, MO 63130, USA

Abstract

In photosynthetic organisms, photons are captured by light-harvesting antenna complexes, and energy is transferred to reaction centers where photochemical reactions take place. We describe here the isolation and characterization of a fully functional megacomplex composed of a phycobilisome antenna complex and photosystems I and II from the cyanobacterium *Synechocystis* PCC 6803. A combination of in vivo protein cross-linking, mass spectrometry, and time-resolved spectroscopy indicates that the megacomplex is organized to facilitate energy transfer but not intercomplex electron transfer, which requires diffusible intermediates and the cytochrome b_6f complex. The organization provides a basis for understanding how phycobilisomes transfer excitation energy to reaction centers and how the energy balance of two photosystems is achieved, allowing the organism to adapt to varying ecophysiological conditions.

In cyanobacteria and redalgae, phycobilisomes (PBSs) (1–3) absorb light and transfer its energy to chlorophylls in photosystem II (PSII) and photosystem I (PSI), where charge separation occurs. This process of light capture by the PBS greatly expands the natural solar spectrum energy use under varying and sometimes extreme light conditions (4). Although spatial orientations of the chromophores in the PBS and chlorophylls in the reaction centers (RCs) dictate an efficient energy transfer, the exact PBS-RCs interactions are as yet unclear.

To address how the three protein complexes structurally interact, we examined chemically cross-linked PBS, PSII, and PSI by using liquid chromatography and tandem mass spectrometry (LC-MS/MS) (5–8) and analyzed the data by using two different searching methods (9, 10). Application of membrane-permeable, chemical cross-linkers to the living cells essentially captures the weak interactions between these components (5). This is made possible by the introduction of a polyhistidine tag on the C terminus of PSII subunit O

*Corresponding author: blankenship@wustl.edu.

Additional data are available in the supplementary materials. The mass spectrometry proteomics data have been deposited to the ProteomeXchange Consortium (http://proteomecentral.proteomexchange.org) via the PRIDE (Proteomics Identifications Database) partner repository (29) with the data set identifier PXD000545.

Supplementary Materials
www.sciencemag.org/content/342/6162/1104/suppl/DC1
Materials and Methods
Figs. S1 to S20
Tables S1 to S5
References (*30–58*)

(PsbO), in which, without cross-linking reactions, only PSII complexes are isolated (Fig. 1 and fig. S2).

Several observations are consistent with the formation of a larger, multicomponent complex. Key components from both PSII and PSI are present as per immunological analysis (fig. S4, A and B); oxygen evolution (PSII) and oxygen consumption (PSI) activities were observed (table S2); not only PBS but PSII and PSI components (table S3) are also present, as demonstrated by LC-MS/MS; additionally, multiple cross-linking occurs between PBS-PSII and PBS-PSI (see below). PSII isolation using affinity chromatography is routine and substantially reduces PSI contamination (fig. S5, A and B) (5). The blue-green band collected from the preparation (fig. S3A) shows characteristic fluorescence emission peaks from PBS, PSII (691 nm), and PSI (720 nm) (fig. S5). Taken together, these observations indicate that we have isolated a protein complex that contains PBS, PSII, and PSI. Considering the cumulative mass of PBS, PSII, and PSI is in the range of several megadaltons, we named this complex the PBS-PSII-PSI megacomplex (MCL).

LC-MS/MS identified all the major components from PBS, PSII, and PSI (table S3). Systematic analysis of the cross-linked MCL identified 26 protein interlinks (table S4). Notably, five interlinks were consistently found between the PSII components and ApcE (allophycocyanin E), a key component of the PBS (Fig. 2A and table S4F). [The PSII and PSI peptide sequence numbering used in this study (*Synechocystis* 6803) has its basis in the 3ARC and 1JB0 crystal structures, respectively (11, 12).] In PSII, Lys^{227} is in the loop D of PsbB (^{227}K:PsbB) and is cross-linked to ^{87}K:ApcE (Fig. 2A and figs. S6 and S7) (5). ApcE, is a multidomain protein responsible for the assembly of the PBS core (13). The N-terminal portion of ApcE (phycobilinprotein, or PB domain) shares high similarity to ApcA (fig. S8) (14). The PB domain, however, is interrupted by a dispensable PB-loop insertion (13, 15). We also found that ^{23}K:PsbD (or D2) is linked to ^{317}K:ApcE (Fig. 2A). Spatial proximity of ^{23}K:PsbD and ^{227}K:PsbB seems likely (10.4 Å, fig. S9), but the cross-links were not found. Furthermore, both ^{457}K:PsbC and ^{35}K:PsbI are cross-linked to ^{523}K:ApcE, which is located on the Arm 2 domain of ApcE (Fig. 2A). PsbI, a binding partner for PsbA (D1), is known to play an important role in stabilizing PsbC in the PSII assembly process (16).

We identified cross-links between ^{11}K:PsaA (Psa for PSI and Psb for PSII) and ^{48}K:ApcD and between ^{49}K:ApcD and ^{76}K:PsaD (Fig. 2E, table S4), in line with the concept that energy absorbed by the PBS is delivered to PSI as well as to PSII (17, 18). Our results locate ApcD on the edge area of PSI through a domain formed by PsaA and PsaD (Fig. 2C). Additionally, LC-MS/MS analysis showed cross-links between ^{17}K:ApcB and ^{30}K:PsaA and between ^{58}K:ApcB and ^{10}K:PsaD (Fig. 2, D and E; fig. S7; and table S4). These data support a docking model in which ^{17}K:ApcB (β) is from one monomer (ApcDβ), and ^{58}K:ApcB (β) is from another (αβ), instead of from one β subunit (fig. S10). These chemical cross-linking data in combination with results from protein modeling (fig. S10B) support a side-on orientation of the PBS core to PSI through a cove formed by PsaD and PsaA (Fig. 2D). Our structural model predicts a closest distance of about 22 Å from PCB (phycocyanobilin) to the cytoplasmic layer of chlorophylls in the PsaA (fig. S11). Although early studies demonstrated the involvement of ApcD in energy transfer from PBS to PSI (19, 20), the route by which the energy migrates from PBS to PSI has been elusive (21). Docking ApcD onto the cove formed by PsaA and PsaD causes no apparent steric clashes on ferredoxin (fig. S12) (12).

We then applied time-resolved fluorescence (TRF) spectroscopy at 77 K to study energy transfer between structurally coupled components of the MCL (Fig. 3). Two-dimensional TRF profiles and representative TRF spectra taken at various delay times after excitation at 550 nm (Fig. 3, A and B) show three distinct emission bands with maxima of 645, 685, and

720 nm associated with fluorescence from phycocyanin (PC), PSII, and PSI, respectively, suggesting that energy transfer from PBS to both photosystems takes place. TRF of the MCL does not show a signature of APC_{680} (terminal energy emitter) fluorescence as in isolated PBS (fig. S13). This may not be surprising if the MCL is functionally intact. The absence of PBS fluorescence around this region and the almost instantaneous rise of the PSII chlorophyll a (Chl a) fluorescence (Fig. 3C) demonstrate efficient energy transfer from PBS to PSII, consistent with the PBS core sitting directly on top of the PSII dimer (Fig. 2A).

The rise of fluorescence associated with the PSI in MCL is not instantaneous (Fig. 3, C and D) but rather delayed compared with the others (figs. S14 to S20), suggesting that PBS-PSII and PBS-PSI energy transfer rates are different. Emission at ~720 nm originates from excitation traps—clusters of Chl a pigments with the strongest excitonic interactions located in the PsaA and PsaB PSI subunits (22). These traps effectively serve as excitation donors to the P700 dimer at physiological temperatures, demonstrating multi-decay character at 77 K (23, 24) (figs. S18 and S19). If energy transfer from the PBS to PSI is slow, the rise of fluorescence at 720 nm should be delayed in the MCL with respect to the isolated PSI, as is demonstrated by the data in Fig. 3D. The delayed rise of the PSI fluorescence may be associated with decreased PBS-to-PSI excitation-energy transfer owing either to side-on orientation of PBS and PSI or to a chemical cross-linking modification effect. We do not exclude the possibility of energy spillover from PSII (25). (Fig. 3E). However, undetectable long-lived PSI fluorescence (26) may indicate that the delayed rise of PSI fluorescence is associated with slow excitation-energy transfer between the PBS and PSI, as indicated by the structural interactions between PsaA and ApcD (terminal energy emitter) (Fig. 2C).

Previous studies have suggested that physical interactions between the PBS core and PSII and I are essential for efficient excitation energy migration from low-energy allophycocyanin (APC) in the PBS core to Chl a in RCs (20, 27). However, the enigmatic “supercomplex” comprising PBS-RCs has never been consistently detected and isolated (21), owing to weak and easily disrupted interactions between these complexes. Our study demonstrates that if cells are gently cross-linked in vivo, the weak interactions can be captured and identified. The isolated complex contains PSI but not the cytochrome b_6f complex, which connects PSI and PSII by mobile-electron carriers. Thus, the MCL is best considered as an energy-transfer complex that directs excitations to one or the other photosystem (Fig. 3E) and not as a complex that includes the complete electron-transport chain.

The isolation of the MCL allows us to witness the merger of three intensely studied photosynthetic events of light harvesting and two light-driven photochemistry reactions in one module. There are still many unresolved issues, including the molecular mechanism that governs the assembly of the MCL and the means by which the excitation energy is delivered to the two photo-systems by the PBS. For instance, the orange carotenoid protein is directly involved in the fluorescence quenching of PBS and possibly in the regulation of energy transfer between PBS and the photosystems (28).

Supplementary Material

Refer to Web version on PubMed Central for supplementary material.

Acknowledgments

We thank T. Bricker and H. Pakrasi for the HT3 strain, G. Ajlani and D. Kirilovsky for the ΔAB strain, all the other members of the Gross and Blankenship laboratories for collegial discussions, and H. Rohrs and M. Plasencia for help with LC-MS/MS instrumentation. The research was supported by the Photosynthetic Antenna Research Center (PARC), an Energy Frontier Research Center funded by the U.S. Department of Energy (DOE), Office of Basic

Energy Science (grant no. DE-SC 0001035 to R.E.B) and National Institute of General Medical Science (grant no. 8 P41 GM103422-35 to M.L.G). H.L., D.M.N, M.P., and G.H. were funded by the DOE grant, H.Z. was funded equally by the DOE and NIH grants, and instrumentation was made available from both DOE and NIH grants.

References and Notes

1. Gantt E, Conti SF. Brookhaven Symp Biol. 1966; 19:393–405. [PubMed: 5966919]
2. Glazer AN. Annu Rev Biophys Biophys Chem. 1985; 14:47–77. [PubMed: 3924069]
3. de Marsac NT, Cohen-bazire G. Proc Natl Acad Sci USA. 1977; 74:1635–1639. [PubMed: 404640]
4. Chen M, Blankenship RE. Trends Plant Sci. 2011; 16:427–431. [PubMed: 21493120]
5. Materials and methods are available as supplementary materials on *Science* Online.
6. Petrotchenko EV, Borchers CH. Mass Spectrom Rev. 2010; 29:862–876. [PubMed: 20730915]
7. Sinz A. Mass Spectrom Rev. 2006; 25:663–682. [PubMed: 16477643]
8. Zheng C, et al. Mol Cell Proteomics. 2011; 10:M110.006841.
9. Xu H, Freitas MA. Proteomics. 2009; 9:1548–1555. [PubMed: 19235167]
10. Walzthoeni T, et al. Nat Methods. 2012; 9:901–903. [PubMed: 22772729]
11. Umena Y, Kawakami K, Shen JR, Kamiya N. Nature. 2011; 473:55–60. [PubMed: 21499260]
12. Jordan P, et al. Nature. 2001; 411:909–917. [PubMed: 11418848]
13. Houmard J, Capuano V, Colombano MV, Coursin T, Tandeau de Marsac N. Proc Natl Acad Sci USA. 1990; 87:2152–2156. [PubMed: 2107546]
14. Capuano V, Braux AS, Tandeau de Marsac N, Houmard J. J Biol Chem. 1991; 266:7239–7247. [PubMed: 1901865]
15. Ajlani G, Vernotte C. Eur J Biochem. 1998; 257:154–159. [PubMed: 9799114]
16. Dobáková M, Tichy M, Komenda J. Plant Physiol. 2007; 145:1681–1691. [PubMed: 17921338]
17. Bruce D, Biggins J. Biochim Biophys Acta. 1985; 810:295–301.
18. Mullineaux CW. Biochim Biophys Acta. 1992; 1100:285–292.
19. Zhao, J.; Zhou, J.; Bryant, DA. Research in Photosynthesis. Murata, N., editor. Vol. 1. Kluwer Academic Publishers; Dordrecht, Netherlands: 1992. p. 25-32.
20. Glazer AN, Bryant DA. Arch Microbiol. 1975; 104:15–22. [PubMed: 808186]
21. Mullineaux CW. Photosynth Res. 2008; 95:175–182. [PubMed: 17922214]
22. Soukoulis V, Savikhin S, Xu W, Chitnis PR, Struve WS. Biophys J. 1999; 76:2711–2715. [PubMed: 10233085]
23. Gobets B, et al. Biophys J. 2001; 81:407–424. [PubMed: 11423424]
24. Hastings G, Kleinherenbrink FAM, Lin S, Blankenship RE. Biochemistry. 1994; 33:3185–3192. [PubMed: 8136353]
25. Biggins J, Bruce D. Photosynth Res. 1989; 20:1–34. [PubMed: 24425462]
26. Yokono M, Murakami A, Akimoto S. Biochim Biophys Acta. 2011; 1807:847–853. [PubMed: 21496452]
27. Redlinger T, Gantt E. Plant Physiol. 1981; 68:1375–1379. [PubMed: 16662111]
28. Kirilovsky D, Kerfeld CA. Photochem Photobiol Sci. 2013; 12:1135–1143. [PubMed: 23396391]
29. Vizcaíno JA, et al. Nucleic Acids Res. 2013; 41:D1063–D1069. [PubMed: 23203882]

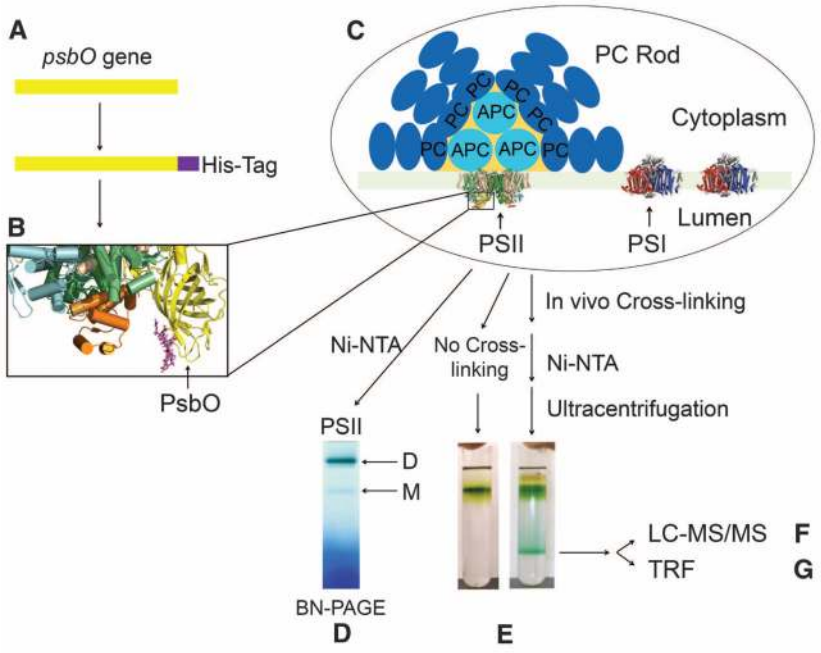

Fig. 1. Schematic outline of the experimental work-flow established for the genetic modification, isolation, and preliminary characterization of the MCL

(**A**) Genetic modification of PsbO protein at C terminus [PsbOH strain (5)]. (**B**) Luminal side of the PSII monomer, indicating the solvent-accessible PsbO C terminus with His_6 tag (purple) introduction. PsbO is colored yellow; PsbU, orange; PsbV, light blue; and loop E of CP43, lime. (**C**) In vivo model of PBS and photosystems. NTA, nitrilotriacetic acid. (**D**) BN-PAGE (blue native polyacrylamide gel electrophoresis) analysis of isolated PSII (PsbOH), dimer (D), and monomer (M). (**E**) Ultracentrifugation isolation of MCL after affinity chromatography. (**F** and **G**) LC-MS/MS and TRF spectroscopy of the MCL.

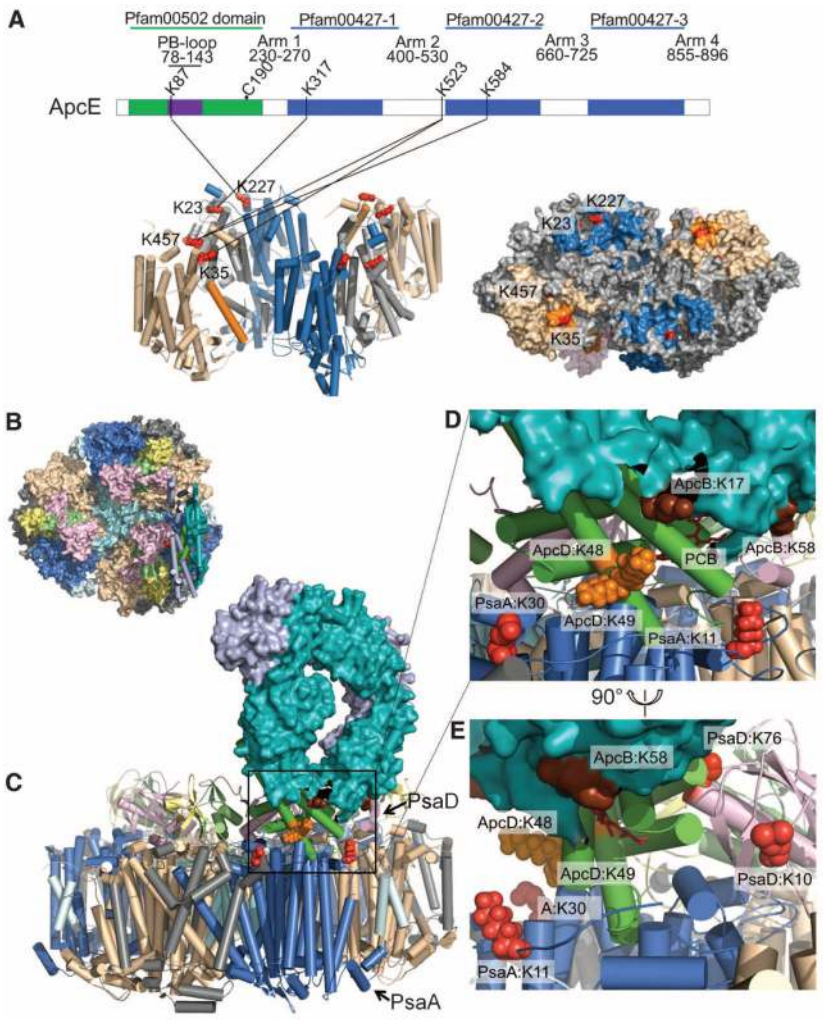

Fig. 2. Identification of interprotein cross-links between PBS and two photosystems

(**A**) ApcE-PSII cross-links. The N-terminal domain of ApcE is the only phycobilin-attached region in linker proteins (Cys^{190}). Five cross-links were found between ApcE and PSII. PsbB, sky blue; PsbC, wheat; PsbD, light gray; PsbI, orange. All lysines (^{227}K:PsbB, ^{457}K:PsbC, ^{35}K:PsbI, and ^{23}K:PsbD) are represented as spheres. (**B**) Docking model of ApcD to PSI trimmer (cytoplasmic view) based on the identified cross-links presented in (**C**). PsaA, marine; PsaB, wheat; PsaC, lime; PsaD, light pink; PsaE, yellow; PsaF, gray; PsaL, cyan; ApcD, green; ApcA, light blue; ApcB, teal. (**D** and **E**) Close-up views of the model shown in (C) and PCB (red sticks). Cross-links were found between ^{48}K:ApcD (orange) and ^{11}K:PsaA, ^{17}K:ApcB and ^{30}K:PsaA, ^{58}K:ApcB and ^{10}K:PsaD, and ^{49}K:ApcD and ^{76}K:PsaD. Lysine residues from PSI, ApcD, and ApcB are presented as red, orange, and chocolate spheres, respectively.

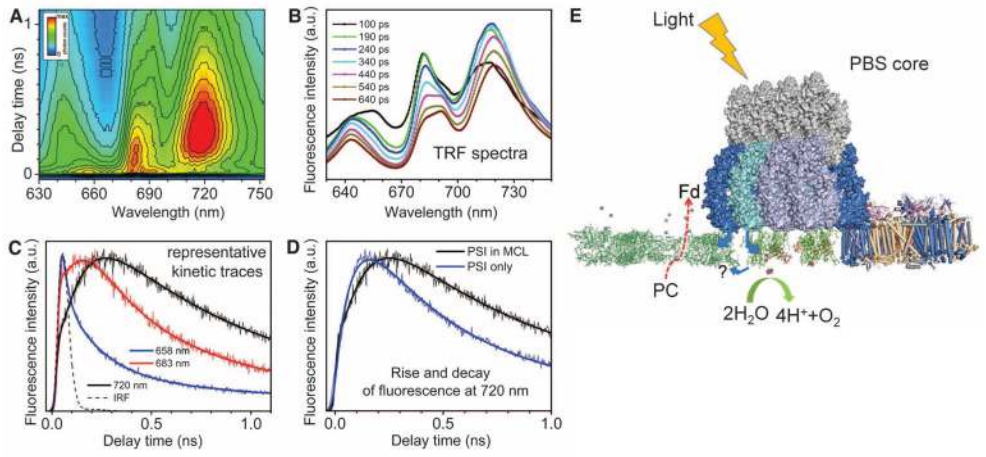

Fig. 3. Time-resolved fluorescence of the MCL at 77 K, fluorescence decay analysis, and model of the PBS-PSII-PSI association in the MCL

(**A**) Two-dimensional profile of TRF recorded in 1-ns time windows after excitation at 550 nm. (**B**) Representative TRF spectra taken at various delay times after excitation. a.u., arbitrary unit. (**C**) Representative fluorescence decay traces taken at three distinct bands (PC, PSII, and PSI) accompanied with fits. IRF, instrument response function. (**D**) Rise and decay of fluorescence at 720 nm (PSI) recorded for the MCL and the isolated PSI. (**E**) The MCL model of the PBS-PSII-PSI association, showing that PSII is fully covered by close association with the PBS core, whereas PSI is associated with ApcD through a side-on orientation.